PAIN

An orally bioavailable MrgprX1-positive allosteric modulator alleviates certain neuropathic pain–related behaviors in humanized mice

Ankit Uniyal[1]†, Niyada Hin[2]†, Chi Zhang[1]†, Qian Xu[3], Qian Huang[1], Ilyas Berhane[2], Ajit G. Thomas[2], John Maragakis[2], Sadakatali Gori[2], Jing Liu[1], Qin Zheng[1], Xiang Cui[1], Qi Peng[3], Jieru Wan[1], Rana Rais[2], Barbara S. Slusher[2], Srinivasa. N. Raja[1], Xinzhong Dong[3,4], Takashi Tsukamoto[2]*, Yun Guan[1,5]*

The human *Mas*-related G protein–coupled receptor X1 (MrgprX1) represents a promising nonopioid analgesic target because of its selective expression in primary nociceptive sensory neurons. Positive allosteric modulators (PAMs) promote receptor signaling, depending on the availability of endogenous ligands, offering physiological selectivity over orthosteric agonists. We developed an orally bioavailable MrgprX1 PAM, 6-tert-butyl-5-(4-chlorophenyl)-4-(2-fluoro-6-(trifluoromethoxy)phenoxy)thieno[2,3-d]pyrimidine (BCFTP). BCFTP selectively potentiated the functional response of MrgprX1 in HEK293 cells, was metabolically stable, and demonstrated a favorable in vitro safety profile. BCFTP was orally bioavailable and distributed into the spinal cords of wild-type mice. BAM22, an endogenous ligand for MrgprX1, was up-regulated in the spinal cord after nerve injury in both wild-type and humanized MrgprX1 mice and was expressed in peptidergic and nonpeptidergic dorsal root ganglion neurons. Oral administration of BCFTP dose-dependently inhibited heat hyperalgesia and spontaneous pain-like behavior but not mechanical hypersensitivity after sciatic chronic constrictive injury (CCI) in MrgprX1 mice. BCFTP did not have analgesic effects in Mrgpr cluster knockout (Mrgpr$^{-/-}$) mice, indicating that the analgesic effects in MrgprX1 mice were MrgprX1 dependent. BCFTP enhanced BAM8-22–induced, MrgprX1-mediated reduction of C-fiber eEPSC amplitudes in spinal lamina II neurons, indicating inhibition of spinal nociceptive synaptic transmission. BCFTP did not induce tolerance or side effects, such as itch, sedation, and motor incoordination, and had no rewarding properties. The mRNAs encoding MrgprX1 and μ-opioid receptors were colocalized in human DRG neurons, and BCFTP synergistically enhanced morphine analgesia in CCI MrgprX1 mice. Our research suggests an approach for developing safer, orally bioavailable MrgprX1 PAM as a nonopioid therapy for neuropathic pain.

INTRODUCTION

Neuropathic pain (NP) remains a substantial clinical challenge (*1*, *2*). Most current therapeutics for NP fail to provide adequate pain relief and induce on-target central side effects, such as sedation, drowsiness, and respiratory depression, limiting their clinical use (*3*, *4*). Although opioid analgesics remain the mainstay of pharmacological treatment for various pain conditions, their utility in chronic pain control is limited due to the development of tolerance and the occurrence of life-threatening side effects (*5*–*9*). This underscores an unmet need for nonopioid therapies to achieve effective and safe pain management.

Primary sensory neurons of the dorsal root ganglion (DRG) play a crucial role in transmitting sensory information to the spinal cord (*10*). Single-cell RNA sequencing (scRNA-seq) studies in patients and corresponding preclinical pain models indicate that DRG neurons undergo profound transcriptional changes after nerve injury (*11*–*15*), and the hyperexcitability of DRG neurons contributes to NP pathophysiology (*11*, *16*–*20*). Clinical studies demonstrate that dynamic modulation of central nociceptive processing is critically dependent on ongoing peripheral afferent input (*21*–*23*). Accordingly, targeting primary nociceptive neurons is an effective strategy for pain treatment and avoiding central side effects.

Human *Mas*-related G protein–coupled receptor X1 (MrgprX1), exclusively expressed by primary sensory neurons (*24*, *25*), has emerged as a potential nonopioid analgesic target (*26*). Bovine adrenal medulla-22 (BAM22) is an endogenous cleavage product of proenkephalin A. A truncated variant lacking the met-enkephalin motif, BAM8-22, activates both MrgprX1 and its rodent functional homolog, MrgprC11 (*27*). However, studying the pharmacological effects of MrgprX1 activation in vivo using conventional rodent models has been difficult, given that human MrgprX1 and MrgprC11 show distinct pharmacological responses to other ligands (*26*, *28*). To address this limitation, we generated transgenic mice in which *MrgprX1* is expressed under the promoter of *MrgprC11* in mouse DRG neurons, referred here to as humanized MrgprX1 mice (*26*), which lack the endogenous *MrgprC11* gene.

Our previous findings showed that the activation of MrgprX1 by BAM8-22 inhibits N-type high-voltage–activated (HVA) calcium current in nociceptive DRG neurons and attenuates spinal nociceptive transmission (*26*). The activation of MrgprX1 and MrgprC11 at the central terminals of DRG neurons that terminate in the spinal cord inhibits NP-like behavior in mice. However, their activation at the peripheral sites triggers itch, presenting a substantial barrier to the translational development of orally active MrgprX1 orthosteric agonists for pain control (*26*, *29*).

[1]Department of Anesthesiology and Critical Care Medicine, Johns Hopkins University School of Medicine, Baltimore, MD 21205, USA. [2]Johns Hopkins Drug Discovery and Department of Neurology, Johns Hopkins University, Baltimore, MD 21205, USA. [3]Solomon H. Snyder Department of Neuroscience, Johns Hopkins University School of Medicine, Baltimore, MD 21205, USA. [4]Howard Hughes Medical Institute, Johns Hopkins University School of Medicine, Baltimore, MD 21205, USA. [5]Department of Neurological Surgery, Johns Hopkins University School of Medicine, Baltimore, MD 21205, USA.
†These authors contributed equally to this work.
*Corresponding author. Email: yguan1@jhmi.edu (Y.G.); ttsukamoto@jhmi.edu (T.T.)

Positive allosteric modulators (PAMs) bind to an allosteric site on the receptor, distinct from the orthosteric site, and lack the intrinsic activity in the absence of a natural ligand. PAMs enhance G protein–coupled receptor (GPCR) signaling in an endogenous ligand availability–dependent manner, thus enabling targeted modulation with reduced side effects while preserving physiological signaling.

Nerve injury up-regulates endogenous BAM22 expression in the spinal cord but not in the skin (*26*, *30*). This offers an opportunity to preferentially boost the activation of spinal MrgprX1 for alleviating pain without inducing itch by using PAMs. This prompted the exploration of small-molecule, orally bioavailable MrgprX1 PAMs to selectively enhance endogenous MrgprX1 signaling in the central terminals of DRG neurons for pain control. To this end, we previously found and reported thieno[2,3-d]pyrimidine–based PAMs, one of which exhibited oral bioavailability in mice and demonstrated in vivo analgesic efficacy in NP models after oral administration in MrgprX1 mice (*30*).

We made further modifications of the lead compound to improve PAM potency, metabolic stability, water solubility, and oral bioavailability, which led to the development of 6-tert-butyl-5-(4-chlorophenyl)-4-(2-fluoro-6-(trifluoromethoxy)phenoxy)thieno[2,3-d]pyrimidine (BCFTP) in this study. We report the pharmacological, behavioral, and electrophysiological mechanistic profiling of BCFTP, an orally bioavailable MrgprX1 PAM with improved potency, as a potential therapeutic agent for NP. Our recent study suggested potential functional interactions between MrgprC11 and μ-opioid receptor (MOR) (*31*). Therefore, we also explored the in vivo functional interplay between BCFTP and morphine in MrgprX1 mice and demonstrated the utility of combined drug treatment for more effective NP management. The current findings pave the way for the development of orally bioavailable MrgprX1 PAMs as nonopioid treatment options for NP.

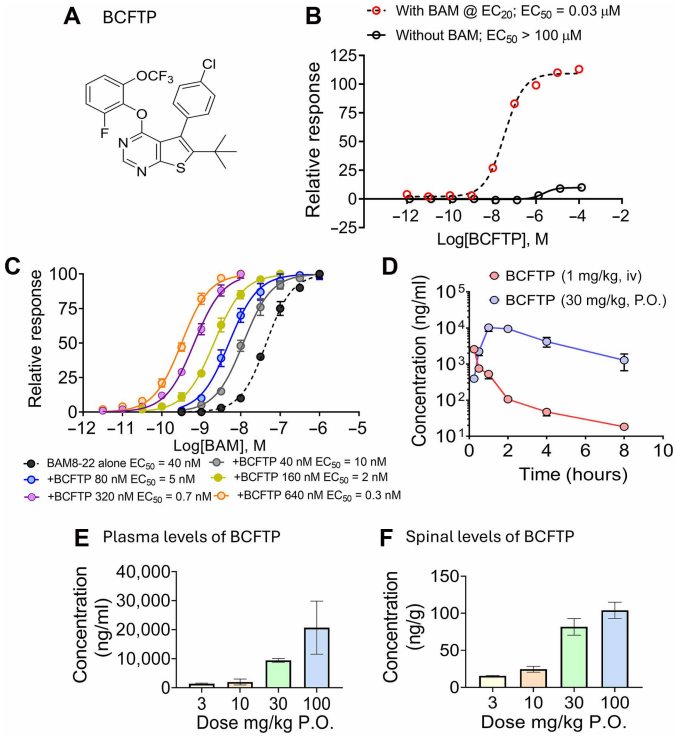

Fig. 1. BCFTP is an orally active and potent MrgprX1-selective PAM. (**A**) The chemical structure of BCFTP. (**B**) MrgprX1 responses to BCFTP with or without BAM8-22 in human embryonic kidney 293 cells stably transfected with human MrgprX1, FLIPR assay. (**C**) Positive allosteric effects of increasing doses of BCFTP on MrgprX1 dose-response to BAM8-22 in FLIPR assay. (**D**) Plasma pharmacokinetics of BCFTP after oral or intravenous administration in wild-type mice. (**E** and **F**) BCFTP abundances in plasma (E) and spinal cord (F) were measured at 2 hours after oral administration at different doses. Data are shown as mean ± SEM, $n = 3$ per group.

RESULTS

BCFTP is a potent and selective MrgprX1 PAM with negligible intrinsic agonist activity

Previous medicinal chemistry efforts identified a series of thieno[2,3-d]pyrimidine-based MrgprX1 PAMs with median effective concentration (EC_{50}) values reaching 100 nM (*30*). BCFTP (Fig. 1A) was developed through additional modifications to the thieno[2,3-d] pyrimidine series, aimed at enhancing PAM potency and metabolic stability. Specifically, a 2-fluoro-6-(trifluoromethoxy)phenoxy group and a 4-chlorophenyl group were incorporated at the 4- and 5-positions, respectively, of the thieno[2,3-d]pyrimidine core scaffold (fig. S1). BCFTP dose-dependently potentiated MrgprX1 response in a fluorescence imaging plate reader (FLIPR) assay elicited by EC_{20} concentration of BAM8-22 with an EC_{50} value of 30 nM (Fig. 1B). In the absence of BAM8-22, BCFTP elicited only 10% of the maximum receptor response achieved by BAM8-22 at the highest concentration (100 μM) tested. The curve shifts produced by various concentrations of BCFTP (0 to 640 nM) indicated a dose-dependent leftward shift of the relative response to the orthosteric MrgprX1 agonist BAM8-22 (Fig. 1C).

BCFTP displays a favorable absorption, distribution, metabolism, and excretion and safety profile in vitro

BCFTP displayed negligible aqueous solubility in phosphate-buffered saline (pH 7.4) and simulated gastric fluid (pH 1.2), although it showed substantially improved aqueous solubility (50 μM) in simulated intestinal fluid (pH 6.8; table S1). BCFTP was metabolically stable in mouse and human liver microsomes for 60 min (table S2). Bidirectional permeability tests indicated that BCFTP is not actively effluxed by P-glycoprotein (table S3).

BCFTP showed no MrgprX2 PAM activity at 5 μM, indicating at least 50-fold selectivity for MrgprX1 (fig. S2). Subsequently, a broader off-target activity profile of BCFTP was evaluated by screening against a panel of 44 selected targets (Eurofins Cerep Safety Screen 44) recommended by major pharmaceutical companies (*32*). BCFTP did not alter the binding of [^{3}H]DAMGO (a MOR agonist) to MOR at 10 μM (>300-fold greater than its EC_{50} value for MrgprX1), ruling out its potential to directly activate or interact with MORs. BCFTP was found to inhibit only three targets (table S4) by more than 50% at this concentration, including human potassium channel hERG (human), which plays an important role in repolarization of cardiac action potential, in a binding assay using [^{3}H]dofetilide. In a hERG patch-clamp assay, the median inhibitory concentration was estimated to be ~28 μM (table S5), nearly 1000-fold higher than its EC_{50} for MrgprX1. Furthermore, BCFTP was confirmed to be negative in the mini-Ames assay, which assesses the mutagenic potential of chemical compounds, at all doses tested in the presence or absence of S9 mix in TA98 or TA100 (table S6). These findings suggest that BCFTP is a highly selective MrgprX1 PAM.

BCFTP is orally bioavailable in mice

Time-dependent PK profiles of BCFTP in mouse plasma are presented in Fig. 1D, and detailed PK parameters are presented in table S7. A single dose of intravenous administration (I.V.) of BCFTP (1 mg/kg) achieved a maximum concentration (C_{max}) of 2.56 μg/ml in plasma at 15 min after injection. The half-life ($t_{1/2}$), volume of distribution (V_d), and clearance (Cl) of BCFTP in plasma were calculated to be 2.49 hours, 1.3 liter/kg, and 6 ml/min per kg, respectively. The overall plasma exposure [area under the curve $(AUC)_{I.V.}$] was calculated to be 2.77 μg·hour per ml. A single dose of oral administration (P.O.) of BCFTP (30 mg/kg) achieved a C_{max} of 10.3 μg/ml in plasma at 1 hour, and $AUC_{0\text{-}t}$ was calculated to be 38.0 μg·hour per ml. BCFTP exhibited excellent oral bioavailability at 46% ($AUC_{P.O.}/AUC_{I.V.}$).

The dose linearity of BCFTP was also evaluated in mouse plasma and spinal cord. Mice were dosed with BCFTP (3, 10, 30, and 100 mg/kg, P.O.), and plasma and spinal cord samples were collected at 2 hours. BCFTP abundance in plasma increased linearly from 1.3 to 20.7 μg/ml with increasing dose (Fig. 1E). BCFTP was detected in the spinal cord, with a spinal cord–to–plasma ratio of 0.5 to 1.2%. However, spinal cord concentrations of BCFTP plateaued at 30 mg/kg with no further substantial increase at 100 mg/kg (Fig. 1F).

Peripheral nerve injury in wild-type and MrgprX1 mice increased BAM22 expression in the lumbar spinal cord and DRGs but not in the skin

We have previously shown that spinal BAM22 expression was increased under NP and inflammatory pain conditions (*26*). Here, we further examined the temporal changes in BAM22 immunoreactivity (IR) in the dorsal horn of the spinal cord in wild-type mice after chronic constrictive injury (CCI) of the sciatic nerve and found a significant increase of BAM22-IR in the ipsilateral dorsal horn at the development (day 7; $P = 0.04$) and maintenance phase (day 14, $P = 0.002$) of NP after CCI, compared with the naïve group (Fig. 2, A and B). Significant ($P < 0.05$) BAM22 up-regulation was also observed in

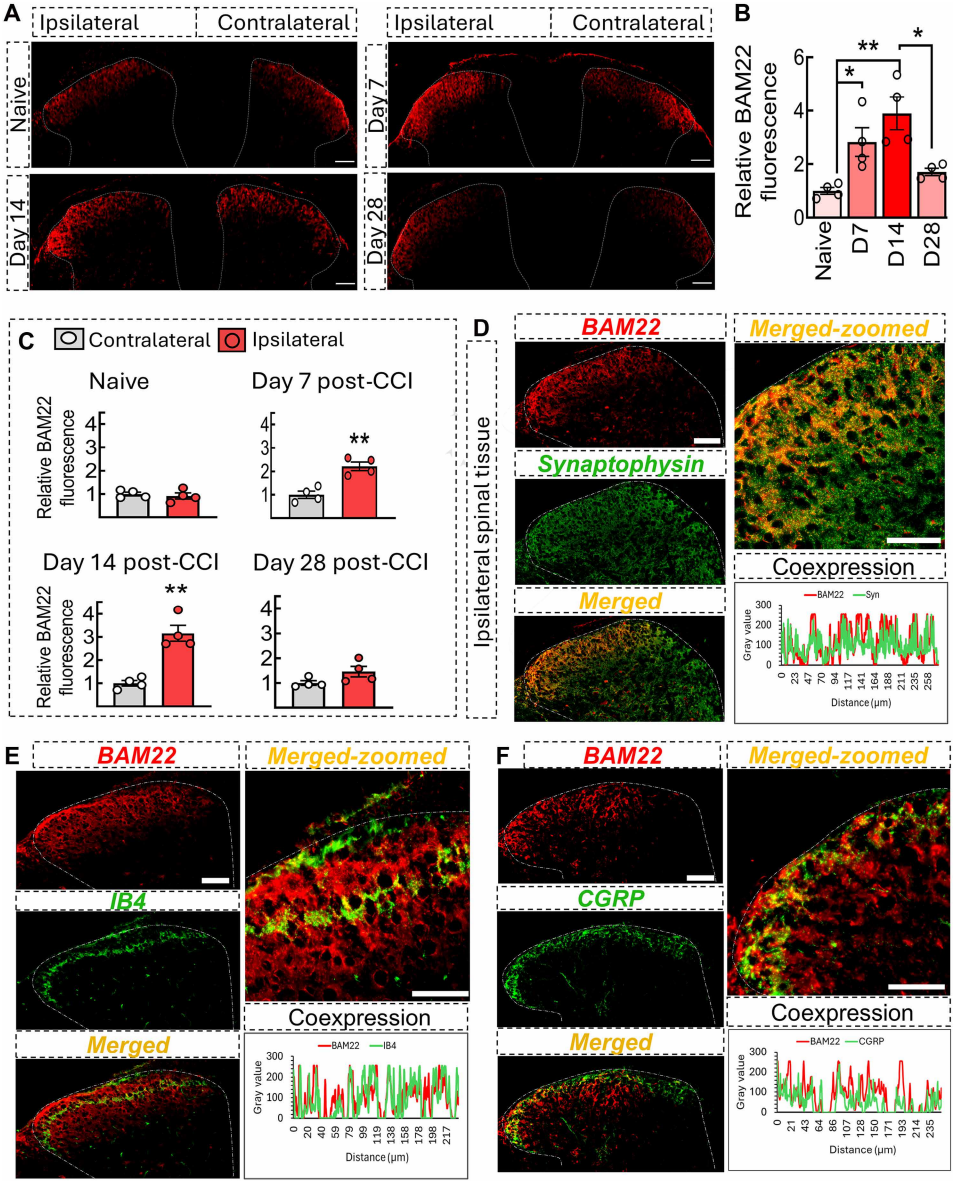

Fig. 2. BAM22-IR was increased in the ipsilateral dorsal horn in wild-type mice after nerve injury. (**A**) Representative immunohistochemical images of naïve and CCI wild-type mouse spinal cord tissue, harvested 7 to 29 days after nerve injury. Tissue sections (thickness, 20 μm) were stained using an antibody against BAM22-IR (red). Scale bar, 100 μm. (**B** and **C**) Quantification of BAM22-IR [from images as in (A), normalized to mean contralateral followed by mean naïve IR] in the ipsilateral dorsal horn at days 7, 14, and 28 post-CCI (B) compared with the respective contralateral side (C). Data are shown as mean ± SEM. (B) One-way ANOVA followed by Tukey's post hoc analysis ($n = 4$ mice per group, two slices per mouse). $^*P < 0.05$ and $^{**}P < 0.01$ versus naïve. D, day. (C) Welch's t test ($n = 4$ mice per group, two slices per mouse). $^{**}P < 0.01$. (**D** to **F**) Representative immunohistochemical image showing the colocalization (yellow) of BAM22 (red) with the presynaptic marker synaptophysin (D), nonpeptidergic marker IB4 (E), or peptidergic marker CGRP (F) in the spinal cord at day 14 post-CCI. The histograms show overlap of BAM22 with the respective cellular markers. The x axis represents the distance between two points analyzed (in micrometers). Scale bars, 40 μm [(D), (E), and (F)].

humanized MrgprX1 mice at day 14 post-CCI, whereas its expression remained undetectable in the hindpaw skin (fig. S3, A to C). Further analysis showed the ipsilateral spinal BAM22-IR was significantly higher on day 7 ($P = 0.002$) and day 14 ($P = 0.001$) post-CCI, compared with the contralateral sides (Fig. 2, A and C). The BAM22-IR expression returned close to preinjury time point and was comparable to that in naïve animals at day 28 post-CCI, suggesting normalized BAM22 expression in the pain-resolving phase of this model.

Coimmunostaining of the lumbar spinal cords of wild-type mice showed that BAM22-IR overlapped with synaptophysin, a presynaptic neuronal marker (Fig. 2D), and with both calcitonin gene-related peptide (CGRP)–positive ($^+$) peptidergic and isolectin B4$^+$ (IB4$^+$) nonpeptidergic terminals of small size DRG neurons (Fig. 2, E and F). Immunostaining of lumbar DRGs from wild-type CCI mice demonstrated that BAM22-IR was coexpressed with β-III tubulin, a neuronal-specific tubulin marker (Fig. 3A). Size distribution analysis showed that BAM22 was predominantly expressed in small (66.2%)– and medium (26.6%)–sized BAM22-expressing neurons but was minimally expressed in large neurons (7.2%; Fig. 3B), which mostly transmit nonnoxious inputs. A significantly higher ($P < 0.001$) abundance of BAM22-IR was observed in the ipsilateral lumbar DRGs compared with that of the contralateral (uninjured) side (Fig. 3C). In line with findings in the spinal cord, BAM22 was expressed in the somata of CGRP$^+$ peptidergic and IB4$^+$ nonpeptidergic nociceptive DRG neurons (Fig. 3, D and E).

Analyzing the dataset from our previous scRNA-seq of DRG tissues from CCI mice showed that *Penk*, the gene encoding the BAM22 precursor peptide proenkephalin, was predominantly expressed not only in peptidergic neurons but also in nonpeptidergic neurons (fig. S4, A and B). *Penk* expression was also increased in the DRGs of CCI mice compared with those of the controls, specifically across the peptidergic neurons (PEP5 cluster) and CCI-induced clusters in injured neurons (fig. S4, C and D). Collectively, these findings suggest that nerve injury may up-regulate *Penk* expression in DRG neurons, leading to an increased downstream production of BAM22, which showed increased abundance both on somata and at the central terminals in the spinal cord.

BCFTP inhibited heat hypersensitivity in MrgprX1 mice after nerve injury and inflammation

To determine the pharmacological effects of BCFTP in vivo, we developed Mrgpr$^{-/-}$; MrgpC11^{MrgprX1} mice (humanized MrgprX1 mice) (*26*). Mrgpr cluster knockout (Mrgpr$^{-/-}$) mice lack an endogenous cluster of mouse Mrgprs (*29*). The MrgprX1 mice are a bacterial artificial chromosome (BAC) transgenic MrgprX1 mouse line in which

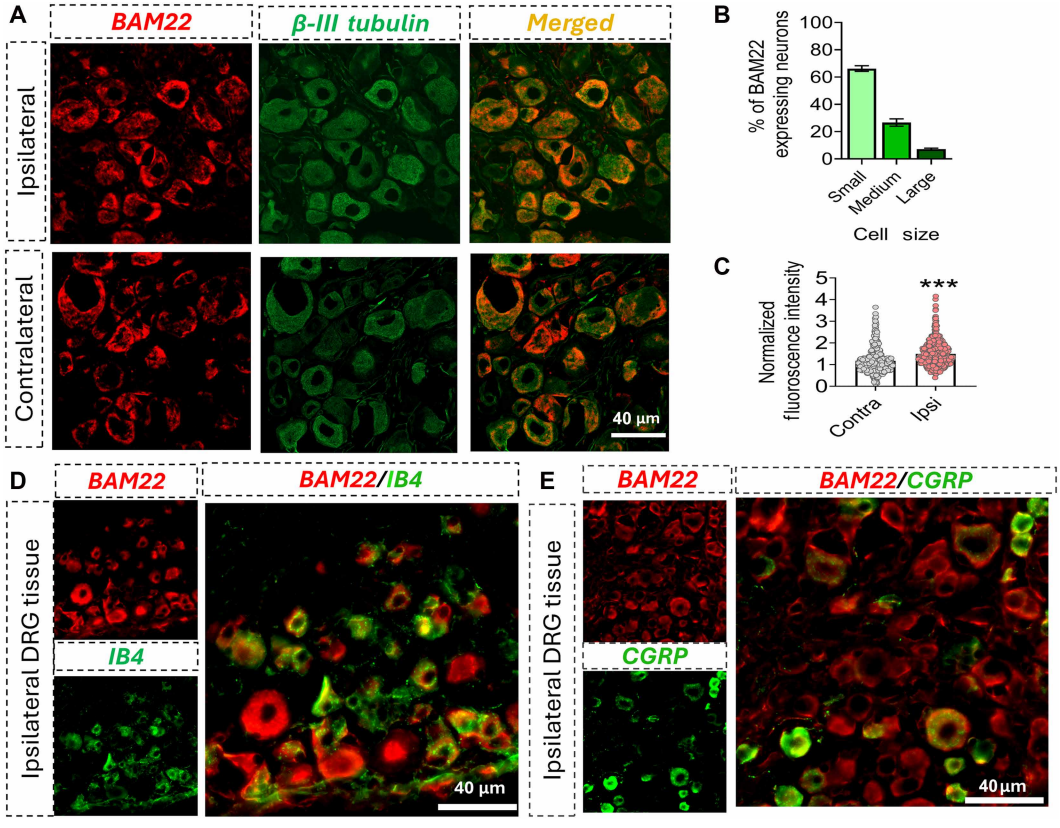

Fig. 3. BAM22-IR was increased in the lumbar DRGs of wild-type mice after CCI. (**A**) Representative immunohistochemical images of naïve and CCI wild-type mouse lumbar DRGs tissue harvested 14 days postinjury. Ipsilateral and contralateral tissue sections (thickness, 10 μm) were stained using antibodies against BAM22-IR (red) and β-III tubulin (green). The picture on the right shows colocalization (yellow). Scale bar, 40 μm. (**B**) Percent distribution of BAM22 across small-, medium-, and large-sized neuron subpopulations, calculated from the total BAM22-expressing ipsilateral DRG neurons of CCI mice ($n = 4$ mice). (**C**) Quantification of average BAM22-IR in individual neurons of the ipsilateral lumbar DRGs of CCI mice, normalized to the mean of the contralateral side. Data are shown as mean ± SEM. Welch's *t* test ($n = 4$ mice). ***$P < 0.001$ versus contralateral. (**D** and **E**) A representative image shows the colocalization (yellow) of BAM22-IR (red) with nonpeptidergic DRG neuronal marker IB4 (C) and peptidergic DRG neuronal marker CGRP (D) in the ipsilateral lumbar DRGs of CCI mice. Scale bars, 40 μm.

the *MrgprX1* expression is driven under the promoter of mouse *MrgprC11* in Mrgpr$^{-/-}$ background (fig. S5).

MrgprX1 mice developed robust heat hyperalgesia at days 12 to 14 post-CCI, as evidenced by a significant decrease of paw withdrawal latencies (PWLs) in the hindpaw ipsilateral to the side of injury, compared with the preinjury baseline ($P < 0.01$; Fig. 4A, top). Oral administration of BCFTP (10, 30, and 100 mg/kg, P.O.) dose-dependently increased PWLs at 1 hour ($P = 0.024$, $P = 0.007$, and $P < 0.001$) and 2 hours ($P < 0.001$, $P < 0.001$, and $P < 0.001$) postdrug, compared with predrug (Fig. 4A, top). The maximum drug effect was observed at 2 hours postdrug. In addition, BCFTP at 30 and 100 mg/kg showed a significant ($P < 0.001$ and $P = 0.04$) inhibition of PWL at 4 hours postdrug, indicating the prolonged antiheat hyperalgesic effect. Gabapentin, a positive control, also significantly ($P < 0.003$) rescued CCI-induced reduction of PWL in MrgprX1 mice (fig. S6). BCFTP at 30- and 100-mg/kg doses ($P = 0.002$ and $P = 0.0064$) increased PWLs in contralateral hind paws of CCI mice at 2 hours postadministration but remained much less than the cut-off value, indicative of mild antiheat nociception (Fig. 4A, bottom).

To quantify the pain inhibitory effect of BCFTP, we calculated the percentage antihyperalgesia score using the formula [1 − (preinjury baseline − postdrug effect)/(preinjury baseline − predrug baseline)] × 100, using ipsilateral PWL data. At a 10-mg/kg dose, BCFTP completely reversed CCI-induced heat hyperalgesia, as indicated by the increased PWL near the preinjury baseline (98%) (Fig. 4B). The higher doses of BCFTP (30 and 100 mg/kg) also showed analgesic ($P = 0.009$

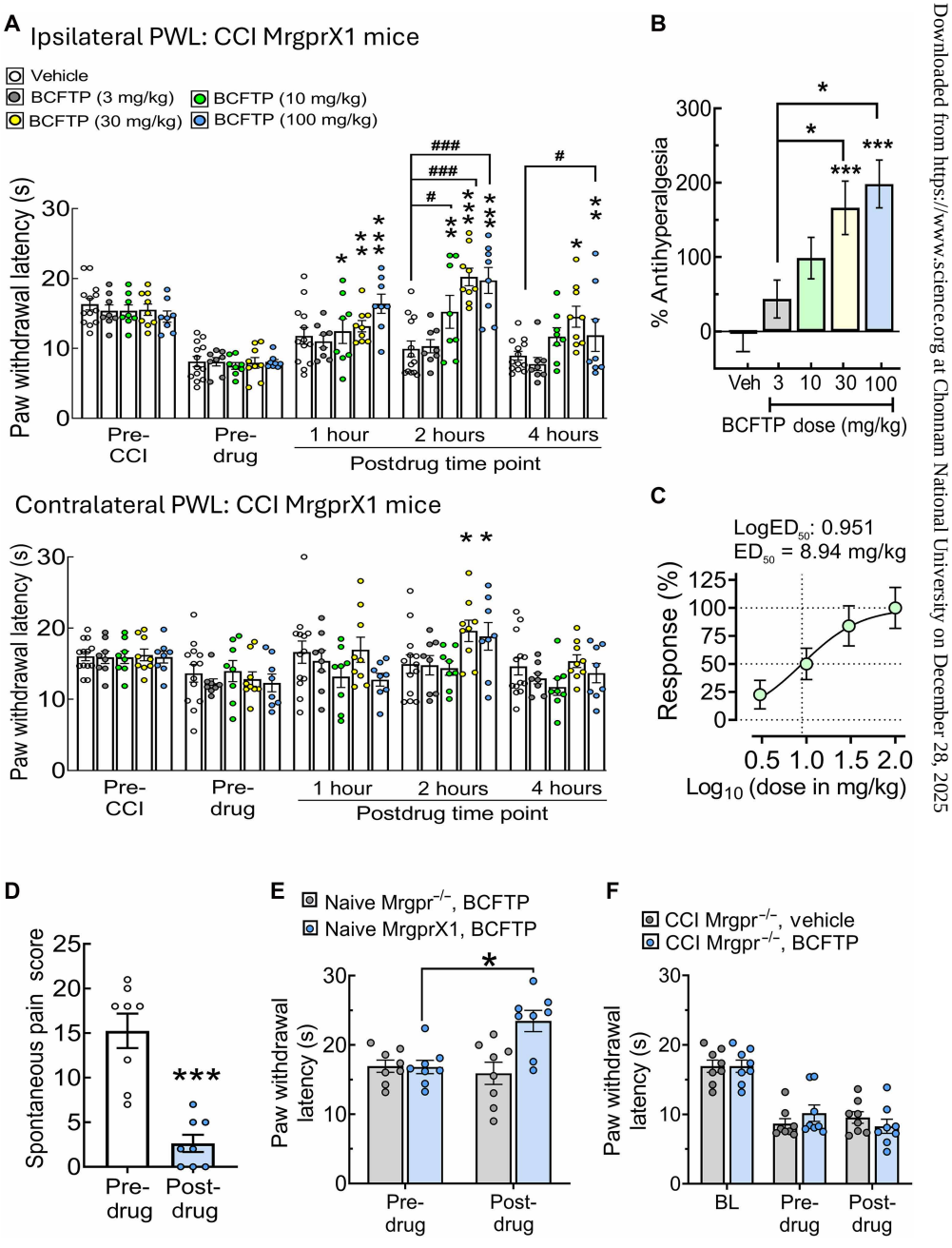

Fig. 4. Oral administration of BCFTP inhibited NP-like behavior in MrgprX1 mice. (**A**) The top shows the ipsilateral PWLs to heat stimuli measured at preinjury, predrug (after CCI injury), and postdrug (1, 2, and 4 hours) for different doses of BCFTP (10, 30, and 100 mg/kg, P.O.) in MrgprX1 mice ($n = 8$ to 13 per group). Bottom shows the contralateral PWLs (uninjured side) after oral administration of BCFTP (30 and 100 mg/kg). Two-way mixed model ANOVA followed by Bonferroni's multiple comparisons analysis. Data are shown as mean ± SEM. $^{*}P < 0.05$, $^{**}P < 0.01$, and $^{***}P < 0.001$ versus predrug; $^{\#}P < 0.05$ and $^{\#\#\#}P < 0.001$ versus the indicated group. (**B**) Reversal of heat hyperalgesia by BCFTP ($n = 8$ to 12 per group). The percentages of antihyperalgesia were calculated using [1 − (preinjury baseline − postdrug effect)/(preinjury baseline − predrug baseline)] × 100. The percentages of antihyperalgesia were calculated at the peak drug effect time point (2 hours post-BCFTP administration), during efficacy testing at day 14 post-CCI. One-way ANOVA followed by Tukey's post hoc analysis. Data are shown as mean ± SEM. (**C**) The BCFTP in vivo dose-response curve with normalized top and bottom values, with the maximum effects observed and the effects without the drug (or vehicle only), respectively. Nonlinear regression analysis, $ED_{50} = 8.94$ mg/kg. The *x* axis represents the dose on a log base 10. (**D**) Spontaneous pain score in SNI-t mice after BCFTP (100 mg/kg, P.O.) treatment ($n = 8$). Paired *t* test. (**E**) Effects of BCFTP on PWLs in naïve Mrgpr$^{-/-}$ and MrgprX1 mice ($n = 8$ per group). (**F**) Ipsilateral PWLs before and after BCFTP oral administration in Mrgpr$^{-/-}$ mice that underwent CCI ($n = 8$ per group). BL, baseline. [(E) and (F)] Data are shown as mean ± SEM. Two-way mixed model ANOVA followed by Bonferroni's multiple comparisons analysis. $^{*}P < 0.05$.

and $P = 0.003$) effects in CCI mice, as indicated by the percentage antihyperalgesia score > 100% (Fig. 4B). The dose-response curve extrapolated from the normalized percentage antihyperalgesia score demonstrated that half maximal effective dose (ED_{50}) of BCFTP was 8.94 mg/kg ($logEC_{50} = 0.95$, hill slope = 1.31; Fig. 4C).

We then investigated the effects of BCFTP on spontaneous pain using MrgprX1 mice with a tibial-spared nerve injury (SNI-t) model, in which sural and common peroneal nerves were transected, whereas the tibial nerve was kept intact. SNI represents a persistent, nonresolving NP model with evoked pain hypersensitivity lasting more than 2 months and robust spontaneous pain-like behavior (*33*–*35*). BCFTP at a 100-mg/kg dose (P.O.) significantly attenuated spontaneous pain in MrgprX1 mice at day 14 post–SNI-t, compared with the predrug ($P < 0.001$; Fig. 4D). In addition, we also observed a significant ($P < 0.01$) up-regulation of BAM-22 IR in the ipsilateral spinal dorsal horns of MrgprX1 mice with SNI-t, as compared with the contralateral side at day 40 postinjury (fig. S7, A and B). To evaluate the effects of BCFTP during the chronic phase of NP, we assessed its effect on heat hyperalgesia at day 30 post–SNI-t. Oral administration of BCFTP (100 mg/kg) significantly attenuated heat hyperalgesia in SNI-t mice, evidenced by increased PWL ($P < 0.001$; fig. S7C) from the predrug baseline.

In addition to NP models, a significant increase ($P < 0.05$) in BAM22-IR was observed in the ipsilateral spinal cords of MrgprX1 mice with intraplantar injection of complete Freund's adjuvant (CFA) (fig. S8, A and B). BCFTP (100 mg/kg, P.O.) significantly attenuated heat hyperalgesia in this CFA-induced inflammatory pain model at 2 hours postdrug administration ($P < 0.05$; fig. S8C).

BCFTP did not inhibit mechanical hypersensitivity in MrgprX1 mice after nerve injury

We next tested the effect of BCFTP on CCI-induced mechanical hypersensitivity using the von Frey test. MrgprX1 mice developed robust mechanical hypersensitivity after CCI, as evidenced by a notable increase in paw withdrawal frequencies (PWFs) to von Frey filament stimuli on the hindpaw ipsilateral to the side of injury, compared with preinjury. However, orally administered BCFTP did not produce significant inhibition of CCI-induced mechanical hypersensitivity in MrgprX1 mice ($P > 0.05$), indicated by comparable PWFs between pre- and postdrug conditions across different doses and time points (fig. S9A). In the high-force (0.4 g) filament test, none of the BCFTP doses except 30 mg/kg (P.O.) showed a significant ($P = 0.016$) effect at 1 hour postdrug (fig. S9B).

We further conducted the Randall-Selitto test to measure mechanical hyperalgesia. We also did not observe a significant ($P = 0.8544$; fig. S9, C and D) inhibition of mechanical hyperalgesia by BCFTP at a 30 mg/kg dose (P.O.), indicated by comparable mechanical thresholds between pre- and postdrug. In contrast, gabapentin at a 100 mg/kg dose (P.O.) reduced CCI-induced mechanical hyperalgesia in both MrgprX1 and $Mrgpr^{-/-}$ mice, indicated by a significant increase of mechanical thresholds ($P = 0.027$ and $P = 0.011$; fig. S9, C and D).

Our previous study showed that intrathecal administration of BAM8-22, a peptide agonist to both MrgprC11 and MrgprX1, significantly inhibited mechanical hypersensitivity in wild-type mice after nerve injury by activating MrgprC11 (*36*). Therefore, we tested whether the direct application of the orthosteric agonist BAM8-22 to the spinal site could inhibit mechanical hypersensitivity in MrgprX1 mice after CCI. However, intrathecal administration of BAM8-22 (5 mM, 5 μl) was not effective in decreasing mechanical PWFs in MrgprX1 and $Mrgpr^{-/-}$ mice after CCI ($P > 0.05$; fig. S9, E and F). Collectively, these observations suggest that neither allosteric nor orthosteric activation of MrgprX1 could alleviate mechanical hypersensitivity in humanized MrgprX1 mice after nerve injury.

Pain inhibitory effects of BCFTP are MrgprX1 dependent

We then used $Mrgpr^{-/-}$ mice to validate the target engagement of BCFTP in vivo. $Mrgpr^{-/-}$ mice lack not only MrgprX1 but also an endogenous cluster of mouse Mrgprs including MrgprC11 (*26*, *29*), allowing us to eliminate potential pharmacological interference from other members of the Mrgpr family. First, we tested the effect of orally administered BCFTP on PWLs using an approximately twice ED_{50} dose (16 mg/kg) in naïve $Mrgpr^{-/-}$ versus MrgprX1 mice. BCFTP significantly increased ($P < 0.001$; Bonferroni's post hoc analysis) thermal PWL in MrgprX1 mice compared with the predrug baseline (Fig. 4E), again suggesting a mild antiheat nociceptive effect at the high dose. This effect of BCFTP was diminished in $Mrgpr^{-/-}$ mice ($P = 0.949$; Fig. 4E).

We further tested the effect of BCFTP (16 mg/kg, P.O.) in $Mrgpr^{-/-}$ mice and MrgprX1 mice after CCI, because the effect of the compound might differ under pathological conditions. The antiheat hyperalgesic effect of BCFTP was abolished in $Mrgpr^{-/-}$ mice ($P = 0.572$; Fig. 4F). In a separate experiment, BCFTP also did not affect spontaneous pain in $Mrgpr^{-/-}$ mice after SNI-t (fig. S10). Collectively, these results confirmed that the pain inhibitory effects of orally administered BCFTP are MrgprX1 dependent.

BCFTP enhanced BAM22-induced inhibition of spinal synaptic transmission in MrgprX1 mice

To examine the neurophysiologic mechanism of pain inhibition by BCFTP, we performed patch-clamp recordings of evoked excitatory postsynaptic currents (eEPSCs) in lamina II dorsal horn neurons of MrgprX1 mice after CCI. The development of NP-like behavior was verified ($P < 0.001$) in these mice before conducting the recording (Fig. 5A). Lumbar (L4-L5) spinal cord slices were used to record eEPSCs in substantia gelatinosa (SG: lamina II) neurons (Fig. 5B). A high-intensity test stimulation (500 μA, 0.1 ms) was applied to the dorsal root to stimulate high-threshold afferent C-fibers.

Bath application of BAM8-22 (0.5 μM) significantly reduced ($P < 0.001$) the amplitudes of high-intensity stimulus-induced C-fiber eEPSCs in SG neurons (Fig. 5, C and D), compared with predrug. Coapplication of BCFTP (5 μM) with BAM8-22 (0.5 μM) significantly ($P < 0.001$) enhanced the inhibition of C-fiber eEPSCs compared with BAM8-22 alone (Fig. 5D). No effect was observed on eEPSCs after bath application of BCFTP (5 μM) alone ($P = 0.907$; Fig. 5E).

Repeated BCFTP treatment did not induce analgesic tolerance in MrgprX1 mice

Tolerance has been associated with the gradual loss of efficacy of several GPCR orthosteric agonists, including morphine and BAM8-22 (*37*–*39*). Therefore, we investigated whether tolerance may also develop to the repeated treatment of BCFTP. We adopted a common tolerance induction protocol (Fig. 6A), which had been validated previously to study tolerance to other GPCR agonists (*38*, *39*). During tolerance induction, MrgprX1 mice received repeated BCFTP or vehicle treatment (P.O., twice daily) for 3 consecutive days, starting on day 12 after CCI. Before tolerance induction, BCFTP (30 mg/kg, P.O.) significantly attenuated heat hyperalgesia in both groups ($P = 0.003$

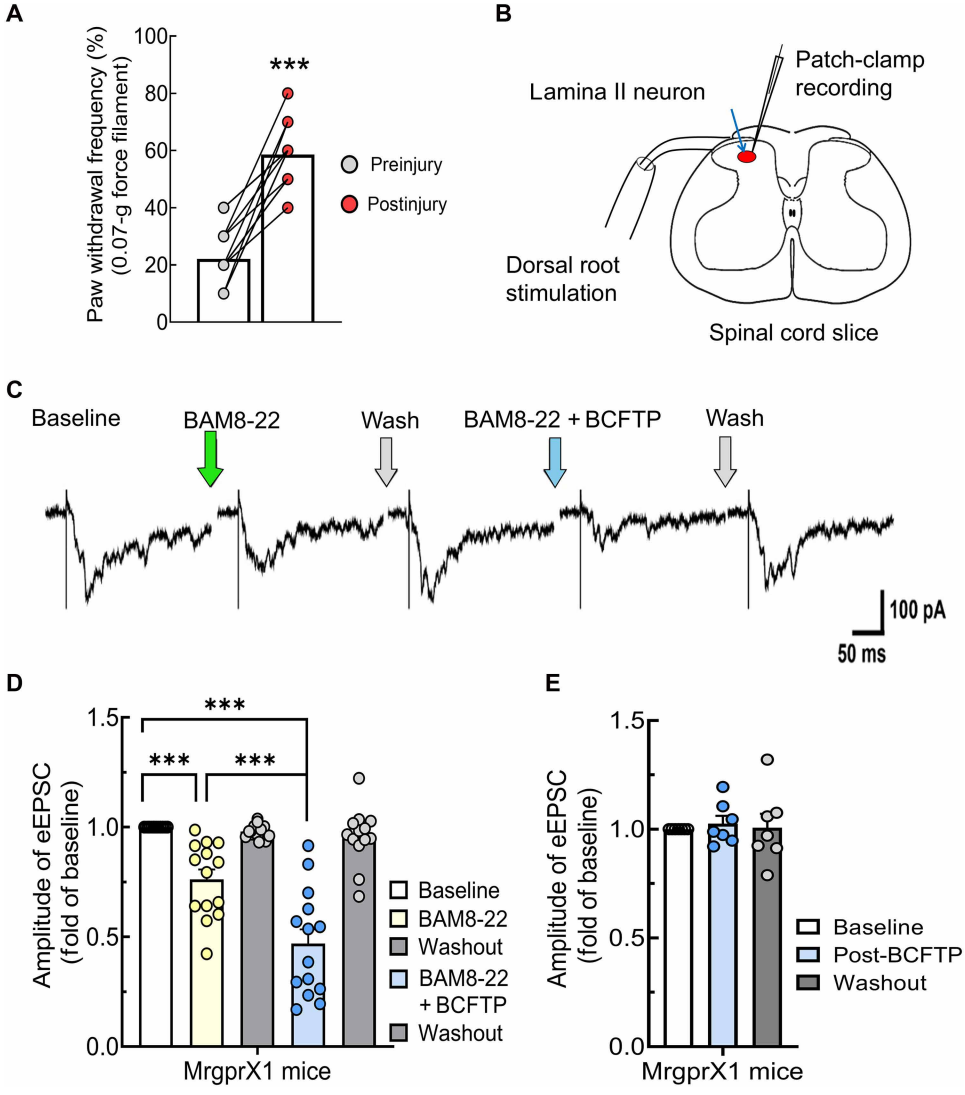

Fig. 5. BCFTP enhanced the inhibition of spinal synaptic transmission by BAM8-22 in superficial dorsal horn neurons of MrgprX1 mice after CCI. (**A**) PWFs to 0.07-g von Frey hair application in MrgprX1 mice before and after CCI. Welch's *t* test. (**B**) Experimental setup of patch-clamp recording from SG neurons in a spinal cord slice. The test stimulation was applied to the dorsal root. (**C**) Representative traces of eEPSCs in response to high-intensity test stimulation (500 μA, 0.1 ms) are shown for baseline, 5 min after BAM8-22 (0.5 μM, bath application), 10-min washout, 5 min after co-application of BAM8-22 (0.5 μM) with BCFTP (5 μM), and 10-min washout in a SG neuron. (**D**) Quantification of the amplitudes of C-fiber eEPSCs in SG neurons from MrgprX1 mice at days 12 to 14 after CCI for a series of drug applications as in (C) (n = 14 mice). (**E**) BCFTP alone did not affect eEPSCs in the spinal cord slice from MrgprX1 mice (n = 7). Data are shown as mean ± SEM. One-way repeated measures ANOVA, with Bonferroni post hoc test. ***P < 0.001 versus baseline and corresponding group.

and $P < 0.001$; Fig. 6B). After the tolerance induction, BCFTP still significantly reduced heat hypersensitivity in both groups ($P = 0.049$ and $P = 0.006$; Fig. 6B), suggesting that repeated allosteric activation of MrgprX1 with BCFTP is not prone to the development of analgesic tolerance under NP conditions.

Oral administration of BCFTP did not produce itch or central side effects

Itch is a common peripheral side effect observed with MrgprC11/X1 agonists, including BAM8-22, because of the activation of these receptors in the skin (*29*, *40*). However, oral administration of BCFTP at a 100-mg/kg dose did not induce itch-like behavior in MrgprX1 mice, as indicated by a comparable number of scratching bouts between the drug and vehicle-administered groups ($P = 0.393$; Fig. 6C).

To assess the central nervous system (CNS) safety profile, we performed open-field and rotarod tests using MrgprX1 mice. In the open-field test, BCFTP (100 mg/kg, P.O.) did not alter total distance compared to the predrug baseline ($P = 0.316$) or the vehicle-administered group ($P = 0.107$; Fig. 6, D and E). In the rotarod test, BCFTP (100 mg/kg, P.O.) also did not impair motor coordination, indicated by comparable fall latencies between the predrug and 1- and 2-hour postdrug values ($P = 0.817$ and $P = 0.467$; Fig. 6F). Moreover, the fall latencies were comparable between BCFTP and vehicle group at 1 hour ($P > 0.999$) and 2 hours ($P = 0.865$) after injection.

The CPP test is a commonly adapted research tool for examining the drug-liking potential of compounds, such as morphine and cocaine, by evaluating the development of preference for the drug-paired chamber (*41*). Naïve MrgprX1 mice did not exhibit a preference for the BCFTP treatment in CPP test ($P > 0.999$; Fig. 6G). Furthermore, BCFTP (100 mg/kg, P.O.) did not induce CPP at day 14 after CCI (fig. S11), suggesting that this compound does not have addictive properties. In contrast, MrgprX1 mice showed a significant preference for morphine compared with vehicle ($P < 0.001$; Fig. 6H). Together, these findings highlight the in vivo safety profile of BCFTP.

Pharmacological interactions between BCFTP and morphine

MrgprC11 and MOR are highly colocalized in small size DRG neurons in wild-type mice, and a pharmacological interaction may occur between their respective agonists (*31*). However, mouse MrgprC11 could not infer the complete pharmacological effects of human

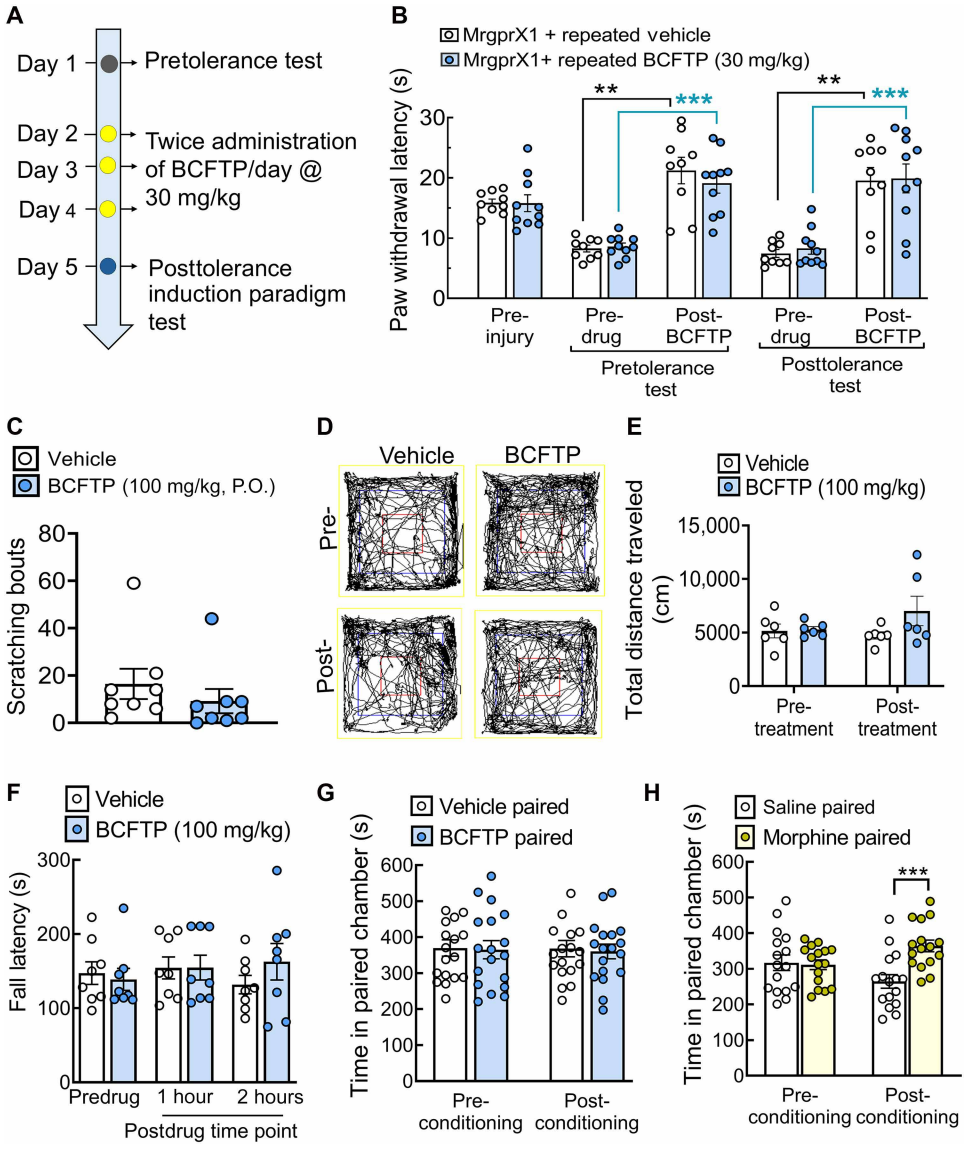

Fig. 6. BCFTP did not produce peripheral and central adverse effects in MrgprX1 mice. (**A**) Protocol for tolerance induction. (**B**) The ipsilateral PWLs were tested at pretolerance and posttolerance conditions in MrgprX1 mice between days 12 and 16 after CCI ($n = 8$ to 10 per group). (**C**) Scratching bouts in MrgprX1 mice treated with BCFTP (100 mg/kg, P.O.) or vehicle. Welch's t test ($n = 8$ per group). (**D**) Representative track maps of MrgprX1 mice before and after drug treatment during open-field tests. (**E**) The total distance traveled by mice in the open field after BCFTP treatment ($n = 6$ per group). (**F**) Rotarod fall latencies at pretreatment and 2 hours after treatment with BCFTP (100 mg/kg, P.O.) or vehicle in MrgprX1 mice ($n = 8$ per group). (**G**) CPP test showing time spent by naïve MrgprX1 mice in vehicle- versus BCFTP (100 mg/kg, P.O.)–paired chambers ($n = 17$ or 18 per group). (**H**) The CPP test shows the time spent by naïve MrgprX1 mice in the vehicle versus morphine (10 mg/kg, sc) paired chamber ($n = 17$ or 18 per group). [(B) to (F)] Data are mean ± SEM. Two-way mixed model ANOVA followed by Bonferroni's multiple comparisons analysis. $^{**}P < 0.01$ and $^{***}P < 0.001$ versus respective predrug values.

MrgprX1. We previously reported that MrgprX1 and MORs may form heteromeric complexes, which may influence each other's functional responses (*31*). Here, using RNAscope analysis of DRG tissue from a human donor with NP, we observed that *MRGPRX1* and *OPRM1* (the gene encoding MOR) are colocalized in the somata of human DRG neurons (Fig. 7A).

We then used in vivo behavioral pharmacology to examine the analgesic interactions between BCFTP and morphine in MrgprX1 mice after CCI. We tested different doses of morphine against CCI-induced heat hyperalgesia (fig. S12, A and B) and identified a subthreshold dose of subcutaneous injection of morphine (1 mg/kg, S.C.), which produced partial but nonsignificant inhibition of heat hyperalgesia (28%, $P = 0.063$), compared to the predrug value. We then rationalized a 1:1 fixed dose combination of morphine and BCFTP. Using the dose-response curve of BCFTP, we identified a dose of 4.5 mg/kg that produced nearly 28% antihyperalgesia. Coadministration of BCFTP (4.5 mg/kg, P.O.) and morphine (1 mg/kg, S.C.) produced significant ($P = 0.011$) inhibition of CCI-induced heat hyperalgesia in MrgprX1 mice compared with predrug (Fig. 7B). The drug combination produced a significantly greater reversal of heat hyperalgesia ($P = 0.025$) than that produced by morphine alone (Fig. 7C). The isobolographic analysis revealed a synergistic interaction between morphine and BCFTP (Fig. 7D). The combination index was calculated to be 0.5, which confirmed the synergic interaction between BCFPT and morphine.

Next, we examined whether BCFTP remains effective in MrgprX1 mice that developed morphine tolerance under NP conditions. Using the same tolerance protocol, repeated morphine (10 mg/kg, S.C.) administration led to the rapid development of analgesic tolerance in MrgprX1 mice after CCI, as evidenced by a significant decrease in the attenuation of decreased PWL by morphine ($P < 0.01$) at posttolerance condition, compared with a pretolerance effect (fig. S12C). BCFTP (30 mg/kg, P.O.) effectively attenuates CCI-induced heat hyperalgesia before and after morphine tolerance ($P < 0.01$ and $P < 0.05$; Fig. 7E). However, the percentage antihyperalgesia score of BCFTP was significantly ($P = 0.039$; Fig. 7F) reduced after morphine

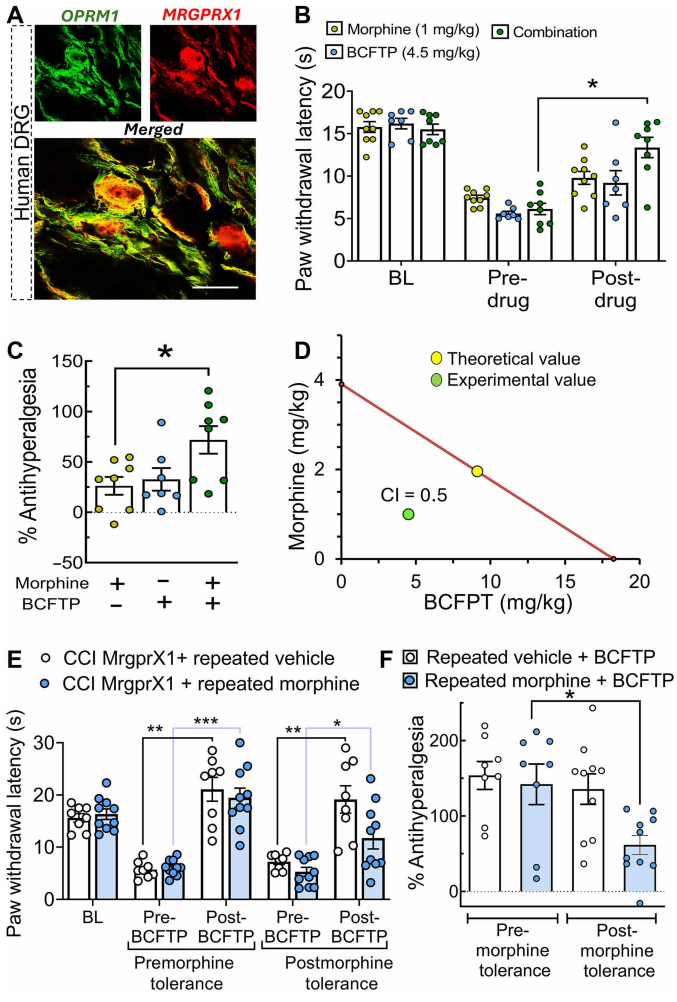

Fig. 7. BCFTP potentiated morphine analgesia but showed cross-tolerance in MrgprX1 mice after CCI. (**A**) Representative RNAscope image showing colocalization of *MRGPRX1* (red) with *OPRM1* (green) signal in human DRG neurons. Scale bar, 50 μm. (**B**) The ipsilateral thermal PWLs before and after oral administration of BCFTP (4.5 mg/kg, P.O.), subcutaneous injection of morphine (1 mg/kg, S.C.), and the combination at 1:1 dose in MrgprX1 mice at days 12 to 14 post-CCI. Data are mean ± SEM. Two-way mixed model ANOVA followed by Bonferroni's multiple comparisons analysis ($n = 8$ to 10 per group). *$P < 0.05$. (**C**) Percentage antihyperalgesia scores for the same groups as in (B). Data are mean ± SEM. One-way ANOVA followed by Tukey's multiple comparisons analysis ($n = 8$ to 10 per group). *$P < 0.05$. (**D**) Isobolographic analysis showing synergistic action between BCFPT and morphine. The brown line joining the *y* axis and the *x* axis shows the theoretical line of additivity representing additive effects. Experimental values below the line of additivity are considered synergistic. CI, combination index. (**E**) Effect of BCFTP on CCI-induced decrease of PWL before and after morphine tolerance in MrgprX1 mice. Data are mean ± SEM. Two-way mixed model ANOVA followed by Tukey's multiple comparisons analysis ($n = 8$ to 11 per group). *$P < 0.05$, **$P < 0.01$, and ***$P < 0.001$. (**F**) % Antihyperalgesia score for the same groups as in (E). Data are mean ± SEM. One-way ANOVA followed by Tukey's multiple comparisons analysis ($n = 8$ to 11 per group). *$P < 0.05$.

tolerance. Specifically, BCFTP produced a 2.6-fold lesser reversal of CCI-induced heat hyperalgesia to preinjury baseline after morphine tolerance, compared with the pretolerance condition (Fig. 7F). In contrast, gabapentin remained effective in increasing PWLs in MrgprX1 CCI mice with morphine tolerance, indicating minimal cross-tolerance between mu-opioids and the gabapentin class of analgesic compounds (fig. S12D).

DISCUSSION

In the present work, we report the development of an orally bioavailable MrgprX1 PAM, BCFTP (fig. S13, A and B). Peripheral nerve injury up-regulated BAM22 expression in the spinal cord and DRG but not in the skin, providing an opportunity to preferentially enhance endogenous activation of MrgprX1 at the central terminals of DRG neurons for NP inhibition using PAM, without eliciting itch. BCFTP selectively activated MrgprX1 and showed optimum solubility in intestinal fluid, microsomal stability, and a good safety profile in vitro. BCFTP was distributed in the spinal cords of mice after oral administration, which is an important site of MrgprX1 agonism–induced pain inhibition, and dose-dependently inhibited heat hyperalgesia and spontaneous pain in MrgprX1 mice after nerve injury. Target engagement studies using Mrgpr$^{-/-}$ mice confirmed that the analgesic effects of BCFTP depended on MrgprX1.

Mechanistically, BCFTP enhanced the BAM8-22–induced inhibition of spinal synaptic transmission mediated by MrgprX1. BCFTP did not produce analgesic tolerance with repeated administration, nor did it cause any observable CNS side effects or itch. These findings support the development of MrgprX1 PAMs as nonopioid therapeutics for the management of NP. In addition, we revealed a positive pharmacological interaction between BCFTP and morphine, suggesting that MrgprX1 PAMs may potentiate morphine analgesia, thereby reducing the required morphine dose to achieve analgesia (opioid sparing).

In rodents, MrgprC11 is predominantly expressed in small-size nonpeptidergic (IB4$^+$) DRG neurons (*42*, *43*). About half of the MrgprC11$^+$ neurons also express CGRP, transient receptor potential vanilloid-1 (TRPV1), and substance-P (*44*). Here, we reported BAM22-IR in both somata and central terminals of small-size peptidergic and nonpeptidergic DRG neurons of wild-type mice, collectively demonstrating the presence of both endogenous ligand and its receptors in nociceptive DRG neurons. The present work is consistent with the previous studies of MrgprC11 in rodents, suggesting that human MrgprX1 at the central terminals of DRG neurons may present a potential analgesic target (*20*, *26*, *30*, *36*, *45*–*48*).

Studies using intrathecal administration of BAM8-22 and ML382 (a nonoral and intrathecally active MrgprX1 PAM) proved that activation of MrgprX1 signaling at the spinal sites effectively inhibits NP-like behavior without inducing itch (*26*, *36*). The up-regulation of BAM22 after peripheral somatosensory insults at the spinal site but not in peripheral tissue provides an opportunity for using PAM to selectively boost the endogenous MrgprX1 agonism at central terminals of DRG neurons after systemic drug administration, thereby avoiding eliciting itch through not engaging peripherally located receptors. We observed a temporal increase in BAM22-IR throughout the time course of NP development and maintenance, suggesting sustained availability of the endogenous agonist and the therapeutic utility of MrgprX1 PAMs for managing NP at different phases. In addition, the up-regulation of spinal BAM22 at the chronic phase in the nonresolving NP model induced by SNI-t and in the inflammatory pain model induced by CFA, consistent with previous reports, highlights the broader therapeutic potential of orally active MrgprX1 PAMs.

To seize this opportunity, we continued our medicinal chemistry efforts on thieno[2,3- d]pyrimidine–based MrgprX1 PAMs, leading

to the development of BCFTP with improved potency; absorption, distribution, metabolism, and excretion (ADME); and safety profile, including favorable oral bioavailability in mice. Oral administration of BCTFP effectively inhibited both heat-evoked and spontaneous pain-like behavior in a MrgprX1-dependent manner. The robust in vivo efficacy of BCTFP may reflect its underestimated dorsal horn concentrations, given that whole-tissue homogenates likely dilute region-specific drug accumulation. In addition, nerve injury may disrupt the blood–spinal cord barrier, altering drug penetration, and the potential involvement of alternative sites of action, such as the sensory ganglia, warrants further investigation.

Previously, intrathecal injection of BAM8-22 inhibited both mechanical and heat hypersensitivity in rats and wild-type mice after nerve injury by activating MrgprC11 (*36*). However, neither BCFTP nor BAM8-22 showed efficacy against mechanical hypersensitivities in MrgprX1 mice after nerve injury. The discrepancy may be due to the lower expression and distribution of MrgprX1 in the DRG of humanized mice versus those of endogenous MrgprC11 in wild-type mice and MrgprC in rats. The MrgprX1 mice were generated using a mouse MrgprC11 BAC clone in which MrgprX1 expression is under the control of MrgprC11 (*26*). However, the BAC clone may not contain all the endogenous enhancers and promoter elements (*49*). In addition, the BAC was randomly inserted in the mouse genome, which can be influenced by the surrounding sequencing (*50*). Last, the MrgprX1 mice have only one copy of the inserted BAC, whereas wild-type mice and rats have two copies of MrgprC. Because of these issues, activation of MrgprX1 in humanized mice may exert an inhibitory effect on thermal but not mechanical pain hypersensitivities due to the lower and narrower expression. Nevertheless, because human DRG neurons are substantially polymodal and have broader MrgprX1 expression (fig. S14) (*25*, *51*–*54*), MrgprX1-targeted therapies may have broader translational effects in humans, including potentially inhibiting mechanical hypersensitivity, which warrants future nonhuman primate study and clinical studies to confirm.

Aligned with previous studies, we demonstrate that BCFTP also potentiates the MrgprX1-mediated inhibition of spinal nociceptive transmission. Among the targets for analgesia, N-type HVA calcium channels play a crucial role at the central terminals of primary sensory neurons in regulating neurotransmitter release into the spinal cord, thereby promoting spinal nociceptive transmission (*45*, *46*, *55*–*58*). MrgprX1 activation by BAM8-22 at spinal sites recruits the Gαi/o pathway, which represents a primary mechanism underlying its inhibition of HVA calcium currents, leading to the inhibition of spinal synaptic transmission (*26*).

Because of its persistent nature, NP often requires prolonged, repeated pharmacological treatment for effective management. However, repeated dosing with exogenous orthosteric agonists of GPCRs, including MOR, MrgprC11, and cannabinoid receptors, can lead to analgesia tolerance (*37*–*39*). The important mechanisms behind the development of tolerance are GPCR down-regulation and predominant coupling of the β-arrestin pathway over heteromeric G proteins, causing receptor desensitization (*37*–*39*, *59*–*62*). However, endogenous ligand-mediated activation of GPCRs was shown to be less liable to develop tolerance. Thus, allosteric activation of GPCRs often maintains the analgesic effects on repeated administration (*63*–*66*). Repeated treatment with BCFTP did not produce analgesic tolerance in a setting that demonstrated tolerance to orthosteric GPCR agonists (*37*, *39*). Further studies are required to explore tolerance using extended time points and different animal models of chronic pain.

BCFTP lacks CNS-associated adverse effects on motor behavior, demonstrating the safety of selective targeting of primary sensory neurons by MrgprX1 PAM. This aligns with previous studies suggesting selective modulation of GPCRs at primary sensory neurons as a safer strategy for pain relief (*16*, *18*, *36*, *39*, *67*). Opioids like morphine have addictive potential and CNS liabilities, thus requiring substantial clinical monitoring and treatment optimization (*68*). In contrast, BCFTP did not produce addiction-like potential because of the restricted nature of its target on primary sensory neurons, suggesting that MrgprX1 PAMs could be used as potentially nonaddictive analgesic therapeutics. The lack of itch with BCFTP administration suggests the selective activation of MrgprX1 signaling in the spinal cord without involving peripheral MrgprX1, unlike orthosteric agonists (*29*, *40*, *44*, *69*). The dual actions of MrgprX1 agonism in inhibiting nociception at central terminals and inducing itch at peripheral terminals of DRG neurons may be associated with different spatial GPCR signaling, coupling of distinct G-proteins and downstream effector proteins, and underlying receptor-ligand structural and functional dynamics (*26*, *40*, *69*–*72*).

BAM8-22 inhibited noxious stimulus-evoked response in superficial spinal dorsal horn neurons in an opioid-independent manner (*73*). However, BCFTP synergistically potentiated the antiheat hyperalgesic effect of morphine in MrgprX1 mice. *MRGPRX1* and *OPRM1* colocalization in human DRG neurons supports the translational potential of their positive pharmacological interaction. Previously, we demonstrated that rodent MrgprC11 also positively modulates MOR function by coinhibiting the cyclic adenosine monophosphate (cAMP) pathway (*31*). Thus, simultaneous activation of G_i-coupled intracellular signaling may partially underlie the potential synergistic action of MrgprX1-MOR interaction. Allosteric activation of MrgprX1 with the coactivation of opioid receptors may provide safer and more effective analgesia by reducing the required dose of opioids. Nevertheless, further studies are warranted to rigorously assess the clinical relevance of this potential opioid-sparing effect across diverse pain models, thereby elucidating the translational potential of the MrgprX1-MOR coactivation strategy.

Our study has some limitations. First, BAM8-22 reduced the chronic morphine treatment–induced cAMP superactivation, minimizing long-term opioid treatment–associated adverse effects (*31*). However, our findings demonstrated that cross-tolerance exists between morphine and MrgprX1 PAM. Opioids also often show cross-tolerance with other GPCR agonists, including cannabinoids (*39*, *74*). Further pharmacokinetic and pharmacodynamic evaluations are needed to optimize the MrgprX1 PAM dose and develop viable MrgprX1 translational therapeutics. Second, we focused primarily on MrgprX1 PAM signaling at the spinal site. Other sites, such as the DRG neuronal soma, may also contribute to the observed effects, which warrant further investigation. Third, the lack of a specific MrgprX1 antibody limited our ability to assess receptor expression and potential cross-interactions with MORs. The current work involved human DRG samples from a single NP patient, which restricted quantitative analyses. Future studies with a larger sample size and the use of different pain models will be essential to validate and translate opioid-sparing strategies based on human MrgprX1 and MOR coactivation.

In conclusion, our study revealed that an orally active MrgprX1-selective PAM can enhance endogenous MrgprX1 signaling, likely at the central terminals of nociceptive DRG neurons, thereby inhibiting NP-like behavior without side effects or tolerance. These findings pave the way for the development of nonopioid analgesics for effective and safe NP control.

MATERIALS AND METHODS

Study design

The main objective of this study was to develop and characterize a PAM of the human MrgprX1 receptor for the treatment of NP. To achieve this goal, we synthesized BCFTP; validated its MrgprX1 PAM activity; characterized its in vitro ADME properties and oral bioavailability in vivo; evaluated its safety profile and receptor engagement using humanized MrgprX1 and Mrgpr$^{-/-}$ mice; assessed its effect on evoked and spontaneous pain behavior after nerve injury; examined the underlying mechanisms of action using patch-clamp electrophysiology of spinal lamina II neurons; and studied its pharmacological interaction with MOR agonist using isobolographic analysis. Animal Research: Reporting of In Vivo Experiments (ARRIVE) 2.0 guidelines were followed for animal experimentation. All animal studies were approved by Johns Hopkins University Animal Care and Use Committee under the protocol approval number MO25M246. The effects of BCFTP on pain-like behaviors were assessed using the CCI, SNI-t, and CFA mouse models of chronic pain. The experimenter was blinded to the mouse genotype and drug treatment to reduce observer bias. All experimental protocols were approved by the Animal Care and Use Committee of Johns Hopkins University School of Medicine, USA. For pharmacological studies, no randomization was done. Human DRG samples were collected from patients suffering from NP who underwent dorsal root ganglionectomy for intractable pain at Johns Hopkins Hospital (IRB00175870). Sample sizes and replicate numbers were determined on the basis of our previous experiments and publications (*16*, *26*, *39*, *47*). Appropriate statistical tests were selected according to variable types and underlying data distribution assumptions. Please see the Supplementary Materials for the detailed methods.

Statistical analysis

ImageJ (National Institutes of Health, USA) was used to analyze the images. Prism 9.0 (GraphPad Inc., San Diego, CA) was used for all statistical analyses. Data were analyzed using the Welch's *t* test or one-way analysis of variance (ANOVA) followed by Tukey's post hoc analysis or two-way ANOVA followed by Bonferroni's multiple comparisons, as appropriate. Statistical significance was set at $P < 0.05$. Data are presented as mean ± SEM. Scattered individual plots were created using GraphPad Prism. All individual-level data are available in data file S1.

Supplementary Materials

The PDF file includes:
Materials and Methods
Figs. S1 to S14
Tables S1 to S7
References (*75*–*79*)

Other Supplementary Material for this manuscript includes the following:
Data file S1
MDAR Reproducibility Checklist

REFERENCES AND NOTES

1. D. Bouhassira, M. Lantéri-Minet, N. Attal, B. Laurent, C. Touboul, Prevalence of chronic pain with neuropathic characteristics in the general population. *Pain* **136**, 380–387 (2008).
2. O. Van Hecke, S. K. Austin, R. A. Khan, B. H. Smith, N. Torrance, Neuropathic pain in the general population: A systematic review of epidemiological studies. *Pain* **155**, 654–662 (2014).
3. N. B. Finnerup, N. Attal, S. Haroutounian, E. McNicol, R. Baron, R. H. Dworkin, I. Gilron, M. Haanpää, P. Hansson, T. S. Jensen, P. R. Kamerman, K. Lund, A. Moore, S. N. Raja, A. S. C. Rice, M. Rowbotham, E. Sena, P. Siddall, B. H. Smith, M. Wallace, Pharmacotherapy for neuropathic pain in adults: A systematic review and meta-analysis. *Lancet Neurol.* **14**, 162–173 (2015).
4. M. Thouaye, I. Yalcin, Neuropathic pain: From actual pharmacological treatments to new therapeutic horizons. *Pharmacol. Ther.* **251**, 108546 (2023).
5. D. Kheirabadi, D. Minhas, R. Ghaderpanah, D. J. Clauw, Problems with opioids beyond misuse. *Best Pract. Res. Clin. Rheumatol.* **38**, 101935 (2024).
6. B. R. Varga, J. M. Streicher, S. Majumdar, Strategies towards safer opioid analgesics—A review of old and upcoming targets. *Br. J. Pharmacol.* **180**, 975–993 (2023).
7. N. D. Volkow, C. Blanco, The changing opioid crisis: Development, challenges and opportunities. *Mol. Psychiatry* **26**, 218–233 (2021).
8. B. Zedler, L. Xie, L. Wang, A. Joyce, C. Vick, J. Brigham, F. Kariburyo, O. Baser, L. Murrelle, Development of a risk index for serious prescription opioid-induced respiratory depression or overdose in Veterans' Health Administration patients. *Pain Med.* **16**, 1566–1579 (2015).
9. G. W. Pasternak, S. R. Childers, Y.-X. Pan, Emerging insights into mu opioid pharmacology. *Handb. Exp. Pharmacol.* **258**, 89–125 (2020).
10. K. Meacham, A. Shepherd, D. P. Mohapatra, S. Haroutounian, Neuropathic pain: Central vs. peripheral mechanisms. *Curr. Pain Headache Rep.* **21**, 1–11 (2017).
11. W. Renthal, I. Tochitsky, L. Yang, Y. C. Cheng, E. Li, R. Kawaguchi, D. H. Geschwind, C. J. Woolf, Transcriptional reprogramming of distinct peripheral sensory neuron subtypes after axonal Injury. *Neuron* **108**, 128–144.e9 (2020).
12. A. M. Barry, N. Zhao, X. Yang, D. L. Bennett, G. Baskozos, Deep RNA-seq of male and female murine sensory neuron subtypes after nerve injury. *Pain* **164**, 2196–2215 (2023).
13. C. Zhang, M. W. Hu, X. W. Wang, X. Cui, J. Liu, Q. Huang, X. Cao, F. Q. Zhou, J. Qian, S. Q. He, Y. Guan, scRNA-sequencing reveals subtype-specific transcriptomic perturbation in DRG neurons of PirtEGFPf mice in neuropathic pain condition. *eLife* **11**, e76063 (2022).
14. P. R. Ray, S. Shiers, J. P. Caruso, D. Tavares-Ferreira, I. Sankaranarayanan, M. L. Uhelski, Y. Li, R. Y. North, C. Tatsui, G. Dussor, M. D. Burton, P. M. Dougherty, T. J. Price, RNA profiling of human dorsal root ganglia reveals sex differences in mechanisms promoting neuropathic pain. *Brain* **146**, 749–766 (2023).
15. G. Baskozos, J. M. Dawes, J. S. Austin, A. Antunes-Martins, L. McDermott, A. J. Clark, T. Trendafilova, J. G. Lees, S. B. McMahon, J. S. Mogil, C. Orengo, D. L. Bennett, Comprehensive analysis of long noncoding RNA expression in dorsal root ganglion reveals cell-type specificity and dysregulation after nerve injury. *Pain* **160**, 463–485 (2019).
16. A. Barpujari, N. Ford, S. Q. He, Q. Huang, C. Gaveriaux-Ruff, X. Dong, Y. Guan, S. Raja, Role of peripheral sensory neuron mu-opioid receptors in nociceptive, inflammatory, and neuropathic pain. *Reg. Anesth. Pain Med.* **45**, 907–916 (2020).
17. G. Landmann, L. Stockinger, B. Gerber, J. Benrath, M. Schmelz, R. Rukwied, Local hyperexcitability of C-nociceptors may predict responsiveness to topical lidocaine in neuropathic pain. *PLOS ONE* **17**, e0271327 (2022).
18. N. C. Ford, A. Barpujari, S. Q. He, Q. Huang, C. Zhang, X. Dong, Y. Guan, S. N. Raja, Role of primary sensory neurone cannabinoid type-1 receptors in pain and the analgesic effects of the peripherally acting agonist CB-13 in mice. *Br. J. Anaesth.* **128**, 159–173 (2022).
19. A. S. Yekkirala, D. P. Roberson, B. P. Bean, C. J. Woolf, Breaking barriers to novel analgesic drug development. *Nat. Rev. Drug Discov.* **16**, 545–564 (2017).
20. A. Uniyal, V. Tiwari, T. Tsukamoto, X. Dong, Y. Guan, S. N. Raja, Targeting sensory neuron GPCRs for peripheral neuropathic pain. *Trends Pharmacol. Sci.* **44**, 1009–1027 (2023).
21. R. H. Gracely, S. A. Lynch, G. J. Bennett, Painful neuropathy: Altered central processing maintained dynamically by peripheral input. *Pain* **51**, 175–194 (1992).
22. R. Staud, S. Nagel, M. E. Robinson, D. D. Price, Enhanced central pain processing of fibromyalgia patients is maintained by muscle afferent input: A randomized, double-blind, placebo-controlled study. *Pain* **145**, 96–104 (2009).
23. S. Haroutounian, L. Nikolajsen, T. F. Bendtsen, N. B. Finnerup, A. D. Kristensen, J. B. Hasselstrøm, T. S. Jensen, Primary afferent input critical for maintaining spontaneous pain in peripheral neuropathy. *Pain* **155**, 1272–1279 (2014).
24. A. Klein, H. J. Solinski, N. M. Malewicz, H. F. Ieong, E. I. Sypek, S. G. Shimada, T. V. Hartke, M. Wooten, G. Wu, X. Dong, M. A. Hoon, R. H. La Motte, M. Ringkamp, Pruriception and neuronal coding in nociceptor subtypes in human and nonhuman primates. *eLife* **10**, e64506 (2021).
25. H. Yu, D. Usoskin, S. S. Nagi, Y. Hu, J. Kupari, O. Bouchatta, S. L. Cranfill, M. Gautam, Y. Su, Y. Lu, J. Wymer, M. Glanz, P. Albrecht, H. Song, G.-L. Ming, S. Prouty, J. Seykora, H. Wu, M. Ma, F. L. Rice, H. Olausson, P. Ernfors, W. Luo, Single-soma deep RNA sequencing of human dorsal root ganglion neurons reveals novel molecular and cellular mechanisms underlying somatosensation. bioRxiv 533207 [Preprint] (2023). https://doi.org/10.1101/2023.03.17.533207.
26. Z. Li, P. Y. Tseng, V. Tiwari, Q. Xu, S. Q. He, Y. Wang, Q. Zheng, L. Han, Z. Wu, A. L. Blobaum, Y. Cui, V. Tiwari, S. Sun, Y. Cheng, J. H. Y. Huang-Lionnet, Y. Geng, B. Xiao, J. Peng, C. Hopkins, S. N. Raja, Y. Guan, X. Dong, Targeting human Mas-related G protein-coupled receptor X1 to inhibit persistent pain. *Proc. Natl. Acad. Sci. U.S.A.* **114**, E1996–E2005 (2017).

27. P. M. C. Lembo, E. Grazzini, T. Groblewski, D. O'Donnell, M.-O. Roy, J. Zhang, C. Hoffert, J. Cao, R. Schmidt, M. Pelletier, M. Labarre, M. Gosselin, Y. Fortin, D. Banville, S. H. Shen, P. Ström, K. Payza, A. Dray, P. Walker, S. Ahmad, Proenkephalin A gene products activate a new family of sensory neuron–specific GPCRs. *Nat. Neurosci.* **5**, 201–209 (2002).
28. H. J. Solinski, T. Gudermann, A. Breit, Pharmacology and signaling of MAS-related G protein–coupled receptors. *Pharmacol. Rev.* **66**, 570–597 (2014).
29. Q. Liu, Z. Tang, L. Surdenikova, S. Kim, K. N. Patel, A. Kim, F. Ru, Y. Guan, H.-J. Weng, Y. Geng, B. J. Undem, M. Kollarik, Z.-F. Chen, D. J. Anderson, X. Dong, Sensory neuron-specific GPCR Mrgprs are itch receptors mediating chloroquine-induced pruritus. *Cell* **139**, 1353–1365 (2009).
30. I. Berhane, N. Hin, A. G. Thomas, Q. Huang, C. Zhang, V. Veeravalli, Y. Wu, J. Ng, J. Alt, C. Rojas, H. Hihara, M. Aoki, K. Yoshizawa, T. Nishioka, S. Suzuki, S. Q. He, Q. Peng, Y. Guan, X. Dong, S. N. Raja, B. S. Slusher, R. Rais, T. Tsukamoto, Thieno[2,3-d]pyrimidine-based positive allosteric modulators of human mas-related G protein-coupled receptor X1 (MRGPRX1). *J. Med. Chem.* **65**, 3218–3228 (2022).
31. S.-Q. He, Q. Xu, V. Tiwari, F. Yang, M. Anderson, Z. Chen, S. A. Grenald, S. N. Raja, X. Dong, Y. Guan, Oligomerization of MrgC11 and μ-opioid receptors in sensory neurons enhances morphine analgesia. *Sci. Signal.* **11**, eaao3134 (2018).
32. J. Bowes, A. J. Brown, J. Hamon, W. Jarolimek, A. Sridhar, G. Waldron, S. Whitebread, Reducing safety-related drug attrition: The use of in vitro pharmacological profiling. *Nat. Rev. Drug Discov.* **11**, 909–922 (2012).
33. Q. Zheng, W. Xie, D. D. Lückemeyer, M. Lay, X.-W. Wang, X. Dong, N. Limjunyawong, Y. Ye, F.-Q. Zhou, J. A. Strong, J.-M. Zhang, X. Dong, Synchronized cluster firing, a distinct form of sensory neuron activation, drives spontaneous pain. *Neuron* **110**, 209–220.e6 (2022).
34. I. Decosterd, C. J. Woolf, Spared nerve injury: An animal model of persistent peripheral neuropathic pain. *Pain* **87**, 149–158 (2000).
35. J. Cichon, L. Sun, G. Yang, Spared nerve injury model of neuropathic pain in mice. *Bio Protoc.* **8**, e2777 (2018).
36. S.-Q. He, Z. Li, Y.-X. Chu, L. Han, Q. Xu, M. Li, F. Yang, Q. Liu, Z. Tang, Y. Wang, N. Hin, T. Tsukamoto, B. Slusher, V. Tiwari, R. Shechter, F. Wei, S. N. Raja, X. Dong, Y. Guan, MrgC agonism at central terminals of primary sensory neurons inhibits neuropathic pain. *Pain* **155**, 534–544 (2014).
37. Q. Huang, N. C. Ford, X. Gao, Z. Chen, R. Guo, S. N. Raja, Y. Guan, S. He, Ubiquitin-mediated receptor degradation contributes to development of tolerance to MrgC agonist–induced pain inhibition in neuropathic rats. *Pain* **162**, 1082–1094 (2021).
38. S.-Q. He, F. Yang, F. M. Perez, Q. Xu, R. Shechter, Y.-K. Cheong, A. F. Carteret, X. Dong, S. M. Sweitzer, S. N. Raja, Y. Guan, Tolerance develops to the antiallodynic effects of the peripherally acting opioid loperamide hydrochloride in nerve-injured rats. *Pain* **154**, 2477–2486 (2013).
39. G. Limerick, A. Uniyal, N. Ford, S. He, S. A. Grenald, C. Zhang, X. Cui, E. Sivanesan, X. Dong, Y. Guan, S. N. Raja, Peripherally restricted cannabinoid and mu-opioid receptor agonists synergistically attenuate neuropathic mechanical hypersensitivity in mice. *Pain* **165**, 2563–2577 (2024).
40. P. Sikand, X. Dong, R. H. LaMotte, BAM8-22 peptide produces itch and nociceptive sensations in humans independent of histamine release. *J. Neurosci.* **31**, 7563–7567 (2011).
41. T. M. Tzschentke, Review on CPP: Measuring reward with the conditioned place preference (CPP) paradigm: Update of the last decade. *Addict. Biol.* **12**, 227–462 (2007).
42. S. Q. He, L. Han, Z. Li, Q. Xu, V. Tiwari, F. Yang, X. Guan, Y. Wang, S. N. Raja, X. Dong, Y. Guan, Temporal changes in MrgC expression after spinal nerve injury. *Neuroscience* **261**, 43–51 (2014).
43. M. J. Zylka, X. Dong, A. L. Southwell, D. J. Anderson, Atypical expansion in mice of the sensory neuron-specific Mrg G protein-coupled receptor family. *Proc. Natl. Acad. Sci. U.S.A.* **100**, 10043–10048 (2003).
44. H. R. Steele, Y. Xing, Y. Zhu, H. B. Hilley, K. Lawson, Y. Nho, T. Niehoff, L. Han, MrgprC11$^+$ sensory neurons mediate glabrous skin itch. *Proc. Natl. Acad. Sci. U.S.A.* **118**, e2022874118 (2021).
45. Z. Li, S.-Q. He, Q. Xu, F. Yang, V. Tiwari, Q. Liu, Z. Tang, L. Han, Y.-X. Chu, Y. Wang, N. Hin, T. Tsukamoto, B. Slusher, X. Guan, F. Wei, S. N. Raja, X. Dong, Y. Guan, Activation of MrgC receptor inhibits N-type calcium channels in small-diameter primary sensory neurons in mice. *Pain* **155**, 1613–1621 (2014).
46. Z. Li, S.-Q. He, P.-Y. Tseng, Q. Xu, V. Tiwari, F. Yang, B. Shu, T. Zhang, Z. Tang, S. N. Raja, Y. Wang, X. Dong, Y. Guan, The inhibition of high-voltage-activated calcium current by activation of MrgC11 involves phospholipase C-dependent mechanisms. *Neuroscience* **300**, 393–403 (2015).
47. Y. Guan, Q. Liu, Z. Tang, S. N. Raja, D. J. Anderson, X. Dong, Mas-related G-protein–coupled receptors inhibit pathological pain in mice. *Proc. Natl. Acad. Sci. U.S.A.* **107**, 15933–15938 (2010).
48. E. Prchalová, N. Hin, A. G. Thomas, V. Veeravalli, J. Ng, J. Alt, R. Rais, C. Rojas, Z. Li, H. Hihara, M. Aoki, K. Yoshizawa, T. Nishioka, S. Suzuki, T. Kopajtic, S. Chatrath, Q. Liu, X. Dong, B. S. Slusher, T. Tsukamoto, Discovery of benzamidine-and 1-aminoisoquinoline-based human MAS-related G-protein-coupled receptor X1 (MRGPRX1) agonists. *J. Med. Chem.* **62**, 8631–8641 (2019).
49. K. Mogi, H. Tomita, M. Yoshihara, H. Kajiyama, A. Hara, Advances in bacterial artificial chromosome (BAC) transgenic mice for gene analysis and disease research. *Gene* **934**, 149014 (2025).
50. X. W. Yang, S. Gong, An overview on the generation of BAC transgenic mice for neuroscience research. *Curr. Protoc. Neurosci.* **5**, Unit 5.20 (2005).
51. D. Tavares-Ferreira, S. Shiers, P. R. Ray, A. Wangzhou, V. Jeevakumar, I. Sankaranarayanan, A. M. Cervantes, J. C. Reese, A. Chamessian, B. A. Copits, P. M. Dougherty, R. W. Gereau IV, M. D. Burton, G. Dussor, T. J. Price, Spatial transcriptomics of dorsal root ganglia identifies molecular signatures of human nociceptors. *Sci. Transl. Med.* **14**, eabj8186 (2022).
52. S. I. Shiers, I. Sankaranarayanan, V. Jeevakumar, A. Cervantes, J. C. Reese, T. J. Price, Convergence of peptidergic and non-peptidergic protein markers in the human dorsal root ganglion and spinal dorsal horn. *J. Comp. Neurol.* **529**, 2771–2788 (2021).
53. S. Shiers, R. M. Klein, T. J. Price, Quantitative differences in neuronal subpopulations between mouse and human dorsal root ganglia demonstrated with RNAscope in situ hybridization. *Pain* **161**, 2410–2424 (2020).
54. S. J. Middleton, A. M. Barry, M. Comini, Y. Li, P. R. Ray, S. Shiers, A. C. Themistocleous, M. L. Uhelski, X. Yang, P. M. Dougherty, T. J. Price, D. L. Bennett, Studying human nociceptors: From fundamentals to clinic. *Brain* **144**, 1312–1335 (2021).
55. J. E. Hartung, J. K. Moy, E. Loeza-Alcocer, V. Nagarajan, R. Jostock, T. Christoph, W. Schroeder, M. S. Gold, Voltage-gated calcium currents in human dorsal root ganglion neurons. *Pain* **163**, e774–e785 (2022).
56. S. S. Murali, I. A. Napier, S. A. Mohammadi, P. F. Alewood, R. J. Lewis, M. J. Christie, High-voltage-activated calcium current subtypes in mouse DRG neurons adapt in a subpopulation-specific manner after nerve injury. *J. Neurophysiol.* **113**, 1511–1519 (2015).
57. G. W. Zamponi, R. J. Lewis, S. M. Todorovic, S. P. Arneric, T. P. Snutch, Role of voltage-gated calcium channels in ascending pain pathways. *Brain Res. Rev.* **60**, 84–89 (2009).
58. Y.-Q. Cao, Voltage-gated calcium channels and pain. *Pain* **126**, 5–9 (2006).
59. R. I. Desai, G. A. Thakur, V. K. Vemuri, S. Bajaj, A. Makriyannis, J. Bergman, Analysis of tolerance and behavioral/physical dependence during chronic CB1 agonist treatment: Effects of CB1 agonists, antagonists, and noncannabinoid drugs. *J. Pharmacol. Exp. Ther.* **344**, 319–328 (2013).
60. M. K. Piscura, D. E. Sepulveda, M. Maulik, J. Guindon, A. N. Henderson-Redmond, D. J. Morgan, Cannabinoid tolerance in S426A/S430A x β-arrestin 2 knockout double-mutant mice. *J. Pharmacol. Exp. Ther.* **385**, 17–34 (2023).
61. K. H. Muchhala, J. C. Jacob, W. L. Dewey, H. I. Akbarali, Role of β-arrestin-2 in short-and long-term opioid tolerance in the dorsal root ganglia. *Eur. J. Pharmacol.* **899**, 174007 (2021).
62. Z. Zuo, The role of opioid receptor internalization and β-arrestins in the development of opioid tolerance. *Anesth. Analg.* **101**, 728–734 (2005).
63. C. Zhu, X. Lan, Z. Wei, J. Yu, J. Zhang, Allosteric modulation of G protein-coupled receptors as a novel therapeutic strategy in neuropathic pain. *Acta Pharm. Sin. B* **14**, 67–86 (2024).
64. N. T. Burford, M. J. Clark, T. S. Wehrman, S. W. Gerritz, M. Banks, J. O'Connell, J. R. Traynor, A. Alt, Discovery of positive allosteric modulators and silent allosteric modulators of the μ-opioid receptor. *Proc. Natl. Acad. Sci. U.S.A.* **110**, 10830–10835 (2013).
65. R. A. Slivicki, Z. Xu, P. M. Kulkarni, R. G. Pertwee, K. Mackie, G. A. Thakur, A. G. Hohmann, Positive allosteric modulation of cannabinoid receptor type 1 suppresses pathological pain without producing tolerance or dependence. *Biol. Psychiatry* **84**, 722–733 (2018).
66. B. M. Ignatowska-Jankowska, G. L. Baillie, S. Kinsey, M. Crowe, S. Ghosh, R. A. Owens, I. M. Damaj, J. Poklis, J. L. Wiley, M. Zanda, C. Zanato, I. R. Greig, A. H. Lichtman, R. A. Ross, A cannabinoid CB_1 receptor-positive allosteric modulator reduces neuropathic pain in the mouse with no psychoactive effects. *Neuropsychopharmacology* **40**, 2948–2959 (2015).
67. V. Tiwari, F. Yang, S. Q. He, R. Shechter, C. Zhang, B. Shu, T. Zhang, V. Tiwari, Y. Wang, X. Dong, Y. Guan, S. N. Raja, Activation of peripheral μ-opioid receptors by dermorphin [d-Arg2, Lys4] (1-4) amide leads to modality-preferred inhibition of neuropathic pain. *Anesthesiology* **124**, 706–720 (2016).
68. A. D. Kaye, S. Kandregula, J. Kosty, A. Sin, B. Guthikonda, G. E. Ghali, M. K. Craig, A. D. Pham, D. S. Reed, S. A. Gennuso, R. M. Reynolds, K. P. Ehrhardt, E. M. Cornett, R. D. Urman, Chronic pain and substance abuse disorders: Preoperative assessment and optimization strategies. *Best Pract. Res. Clin. Anaesthesiol.* **34**, 255–267 (2020).
69. P.-Y. Tseng, Q. Zheng, Z. Li, X. Dong, MrgprX1 mediates neuronal excitability and itch through tetrodotoxin-resistant sodium channels. *Itch* **4**, e28 (2019).
70. N. Gour, X. Dong, The MRGPR family of receptors in immunity. *Immunity* **57**, 28–39 (2024).
71. D. P. Green, The role of Mrgprs in pain. *Neurosci. Lett.* **744**, 135544 (2021).
72. B. Gan, L. Yu, H. Yang, H. Jiao, B. Pang, Y. Chen, C. Wang, R. Lv, H. Hu, Z. Cao, R. Ren, Mechanism of agonist-induced activation of the human itch receptor MRGPRX1. *PLOS Biol.* **21**, e3001975 (2023).
73. Y. Hong, P. Dai, J. Jiang, X. Zeng, Dual effects of intrathecal BAM22 on nociceptive responses in acute and persistent pain–potential function of a novel receptor. *Br. J. Pharmacol.* **141**, 423–430 (2004).
74. L. R. Gerak, C. Zanettini, W. Koek, C. P. France, Cross-tolerance to cannabinoids in morphine-tolerant rhesus monkeys. *Psychopharmacology* **232**, 3637–3647 (2015).

75. G. J. Bennett, Y.-K. Xie, A peripheral mononeuropathy in rat that produces disorders of pain sensation like those seen in man. *Pain* **33**, 87–107 (1988).
76. K. Hargreaves, R. Dubner, F. Brown, C. Flores, J. Joris, A new and sensitive method for measuring thermal nociception in cutaneous hyperalgesia. *Pain* **32**, 77–88 (1988).
77. R. J. Tallarida, An overview of drug combination analysis with isobolograms. *J. Pharmacol. Exp. Ther.* **319**, 1–7 (2006).
78. R. J. Tallarida, The interaction index: A measure of drug synergism. *Pain* **98**, 163–168 (2002).
79. L. O. Randall, J. J. Selitto, A method for measurement of analgesic activity of inflamed tissue. *Arch. Int. Pharmacodyn. Ther.* **111**, 409–419 (1957).

Acknowledgments
Funding: This study was supported by NIH (Bethesda, Maryland, USA) grants UG3NS115718 (T.T.), R01NS070814 (Y.G.), R01NS110598 (Y.G.), and R01NS117761 (Y.G.) and the Johns Hopkins Institute for Clinical and Translational Research (ICTR), which is funded in part by UL1TR001079 from the National Center for Advancing Translational Sciences (NCATS). This study was also subsidized by a seed grant from Johns Hopkins Blaustein Pain Research Fund (Y.G.) and by the Lerner Family Fund for Pain Research (J.L.). X.D. is an investigator at the Howard Hughes Medical Institute. Animal behavioral studies were facilitated by the Pain Research Core, funded by the Blaustein Fund, and the Neurosurgery Pain Research Institute at Johns Hopkins University. Funders had no role in the study design, data collection, data interpretation, or the decision to submit the work for publication. **Author contributions:** A.U. performed most of the experiments, analyzed and visualized the data, was involved in study design, conceptualization, and discussion, and wrote the first draft of the manuscript. N.H., I.B., A.G., J.M., S.G., and Q.P. synthesized the compound and performed some of the experiments and in vitro and ADME studies. C.Z., Q.X., J.L., X.C., Q.Z., and J.W. performed some of the experiments, including animal surgery, injections, genotyping, tissue preparation, electrophysiology, and data analysis, and contributed to editing the manuscript. Y.G., B.S.S., R.R., T.T., X.D., and S.N.R. contributed to data interpretation, experiment design, discussion, and manuscript editing. Y.G. and T.T. conceived and supervised the project, including funding acquisition, experimental design, implementation, and data analysis and compiled the final manuscript with input from all authors. **Competing interests:** S.N.R. is a consultant for AbbVie and Vertex Pharmaceuticals. Y.G. is a consultant for AlpheraBio LLC. Y.G. received a research award from BioTissue Inc. I.B., N.H., B.S.S., T.T., X.D., and Y.G. are listed as inventors in patent applications filed by Johns Hopkins Technology Ventures covering previously unidentified compositions of MrgprX1 PAMs, including BCFTP. This arrangement has been reviewed and approved by Johns Hopkins University in accordance with its conflict-of-interest policies. **Data and materials availability:** All data associated with this study are present in the paper or the Supplementary Materials. BCFTP, Mrgpr$^{-/-}$ mice, and MrgprX1 mice can be made available to interested researchers through a material transfer agreement with the Johns Hopkins University.

Submitted 24 February 2025
Resubmitted 28 July 2025
Accepted 13 November 2025
Published 17 December 2025
10.1126/scitranslmed.adw9446